The potential to narrow uncertainty in projections of regional precipitation change

Ed Hawkins · Rowan Sutton

Abstract We separate and quantify the sources of uncertainty in projections of regional (∼ 2500 km) precipitation changes for the 21st century using the CMIP3 multi-model ensemble, allowing a direct comparison with a similar analysis for regional temperature changes. For decadal means of seasonal mean precipitation, internal variability is the dominant uncertainty for predictions of the first decade everywhere, and for many regions until the third decade ahead. Model uncertainty is generally the dominant source of uncertainty for longer lead times. Scenario uncertainty is found to be small or negligible for all regions and lead times, apart from close to the poles at the end of the century. For the global mean, model uncertainty dominates at all lead times. The signal-to-noise ratio (S/N) of the precipitation projections is highest at the poles but less than 1 almost everywhere else, and is far lower than for temperature projections. In particular, the tropics have the highest S/N for temperature, but the lowest for precipitation. We also estimate a 'potential S/N' by assuming that model uncertainty could be reduced to zero, and show that, for regional precipitation, the gains in S/N are fairly modest, especially for predictions of the next few decades. This finding suggests that adaptation decisions will need to be made in the context of high uncertainty concerning regional changes in precipitation. The potential to narrow uncertainty in regional temperature projections is far greater. These conclusions on S/N are for the current generation of models; the real signal may be larger or smaller than the CMIP3 multi-model mean. Also note that the S/N for extreme precipitation, which is more relevant for many climate impacts, may be larger than for the seasonal mean precipitation considered here.

Keywords precipitation; uncertainty

1 Introduction

In order to adapt to a changing climate, decision makers require quantitative predictions of climate on regional scales. Such predictions are available from global climate models (GCMs), but they have large uncertainties: for example, for many regions even the sign of the change in mean precipitation is uncertain (e.g., Meehl et al., 2007). This large uncertainty comes from three sources, namely model uncertainty, scenario uncertainty and

Ed Hawkins · Rowan Sutton
NCAS-Climate, Department of Meteorology, University of Reading, Reading, UK. E-mail: e.hawkins@reading.ac.uk

the random, internal variability of climate. Model uncertainty arises from each GCM projecting somewhat different future changes in climate in response to the same radiative forcings, and scenario uncertainty results from the unknown future changes in anthropogenic forcings. Internal climate fluctuations could potentially mask or enhance, for a decade or so, the signal of anthropogenic changes; appreciation of these fluctuations is especially important for decision makers tasked with adapting to a changing climate.

The value for decision making of predictive information depends, to a large extent, on the signal-to-noise ratio of the prediction, i.e. how large is the expected change compared to the uncertainty in the prediction. Thus one key issue for climate prediction is, what is the signal-to-noise ratio for different regions and climate variables? An equally important second question is what is the potential to increase the signal-to-noise ratio, and therefore the value of the predictions, by decreasing the uncertainties? In a previous study Hawkins and Sutton (2009) (hereafter HS09) we addressed both these questions for predictions of surface air temperature change over the twenty first century. Through an analysis of the CMIP3 multi-model ensemble we quantified the signal-to-noise ratio for different regions and lead times, and demonstrated that the uncertainty in predictions of the next few decades is dominated by contributions (especially model uncertainty) that are potentially reducible through progress in climate science.

However, the dominant sources of uncertainty depend on the climate variable of interest. Precipitation change is a key variable for adaptation. Several previous studies have demonstrated that internal variability is a significantly more important factor for predictions of precipitation change than for predictions of temperature change (e.g., Räisänen, 2001, Murphy et al., 2004). This research has also shown that predictions of precipitation change are more consistent (higher signal-to-noise ratio) for some regions than others (e.g., Giorgi and Mearns, 2002; Tebaldi et al., 2004; Murphy et al., 2004; Stainforth et al., 2005; Harris et al., 2006, Giorgi and Bi, 2009). For example, the Mediterranean region is typically predicted to experience significantly drier summers in the future whichever GCM is used. Most recently, Giorgi and Bi (2009) used the CMIP3 multi-model ensemble to estimate the signal-to-noise ratio (S/N) for changes in seasonal mean precipitation. They found that, for a limited number of regions (including the Mediterranean and Central America), the S/N becomes greater than 1 sometime during the 21st century, and thus the sign of the precipitation change is robust across this particular set of GCMs.

In this paper we perform a similar analysis to that of Giorgi and Bi (2009) but using the methodology that we employed in HS09. Using this methodology, we explicitly partition the sources of uncertainty in predictions of regional precipitation change (which was not done by Giorgi and Bi, 2009), and obtain quantitative estimates of the signal-to-noise ratio, which we compare with those of Giorgi and Bi (2009). We then go on to quantify the potential to increase the signal-to-noise ratio through progress in climate science (in particular, improvements in climate models). Because we use the same methodology to analyse precipitation as we used to analyse surface air temperature, we are able to compare and contrast the findings for these two variables.

The paper is structured as follows. Section 2 describes the methods used to separate and quantify the sources of uncertainty. We examine how the contributions to total uncertainty vary for different regions and seasons in Section 3. The robustness of the predictions,

measured by the signal-to-noise ratio is explored in Section 4, and we conclude and discuss the implications of our results in Section 5.

2 Partitioning uncertainty in precipitation projections

We utilise precipitation projections for the 20th and 21st century from fourteen different GCMs, under historical forcings and three different future emissions scenarios (SRES A1B, A2 and B1). The particular GCMs used in the analysis were chosen purely on the basis of data availability, i.e. we used the GCMs for which all three different scenario simulations were available. Although some of the GCMs have several realisations of these simulations, we use just one ensemble member for each GCM to treat all the models equally. Fig. 1 shows the global mean, annual mean precipitation projections for the GCMs used, as a percentage change from the mean of 1971-2000. The thick lines represent the multi-model mean for each emissions scenario. Although the GCMs all predict an increase in global mean precipitation, there is a considerable spread. On regional scales this spread can be far larger (e.g., Meehl et al., 2007).

2.1 Separating the sources of uncertainty

Following HS09 we consider that there are three independent sources of uncertainty in these precipitation projections. Firstly, there is model uncertainty: for the same radiative forcings, different models produce different projections (shown by the spread between similarly coloured lines in Fig. 1). Secondly, there is scenario uncertainty: uncertainty in future radiative forcing causes uncertainty in future climate (demonstrated by the spread in the thick coloured lines in Fig. 1). Thirdly, there are the random, internal fluctuations in climate, which are the 'wiggles' superimposed on the long term trends in each projection.

   These sources of uncertainty are separated and quantified following the methods described by HS09; here we give brief details. Firstly, the percentage change from the mean of 1971-2000 is calculated for each projection[1], and a smooth fourth-order polynomial is fitted for 1950-2099. The decadal mean residuals from these smooth fits for 2000-2099 are considered to represent the internal variability, which is assumed to be constant with lead time[2]. We take the average over all models as our best estimate. The model spread around the mean for each scenario is considered as the model uncertainty, and this is averaged over the three scenarios considered. Finally, the spread between the multi-model means for each scenario is considered as the scenario uncertainty. Each model is assumed to be independent and equally realistic, i.e. no effort is made to weight the models by their ability to simulate historical precipitation changes. The analysis can be repeated for different seasonal means and regions. In all that follows we consider the uncertainties in decadal means.

---

[1] Note that the results are not significantly different if the absolute changes from the mean of 1971-2000 are considered, rather than the percentage changes.

[2] Boer (2009) noted a small increase in decadal variability of precipitation in the tropics for stabilised B1 and A1B scenarios in the CMIP3 ensemble. If we allow the variability to change with time in our analysis, the results are virtually indistinguishable, but for simplicity we assume a constant decadal variability.

In this analysis we assume that the model estimates of internal variability are realistic and that the inter-model spread is representative of the true model uncertainty. We acknowledge that these methods are fairly simple but, as discussed in detail by HS09, we expect that the findings are qualitatively robust, especially for projections of the next few decades. Additionally, Appendix A demonstrates that the methodology described above for estimating the internal variability component of uncertainty from the future scenarios gives similar answers to the variability estimated from the unforced control integrations; this gives us more confidence that our findings are robust.

2.2 Uncertainties in global mean precipitation change

We first consider how the uncertainty in global mean, decadal mean precipitation grows over the 21st century and how this uncertainty is partitioned amongst the three components (Fig. 2a). Throughout the century, model uncertainty (blue) is the dominant contributor, but at the start of the century, internal variability (orange) is important, and scenario uncertainty (green) becomes more important at the end of the century. This dominance of model uncertainty for precipitation can be contrasted with the situation for temperature (Fig. 2b) which shows that scenario uncertainty is more important than model uncertainty from mid-century onwards (also see HS09).

The spread in GCM estimates of the historical changes in precipitation and temperature are shown in grey in Fig. 2, with the mean in white. An observational estimate from the Global Precipitation and Climatology Project (GPCP; Adler et al., 2003) version 2.1 is shown with the black line in Fig. 2a, suggesting that the GCMs may sufficiently represent global decadal variability of precipitation, although the observed record is short and is itself subject to considerable uncertainty. For temperature, the GCM estimates agree well with an estimate from the HadCRUT3 dataset (Brohan et al., 2006), which is shown as the black line in Fig. 2b.

As an alternative representation of the uncertainty in precipitation, Fig. 3a shows the fractional uncertainty (i.e. the uncertainty divided by the expected change), for global, decadal mean precipitation. This representation shows that the smallest fractional uncertainty (or the largest signal-to-noise ratio), occurs around 2070, far later than for temperature, which has the minimum around 2040 (Fig. 3b, also see HS09).

Finally, Fig. 4a shows the *fraction* of the total variance in global mean precipitation projections due to each source of uncertainty, for different lead times in the 21st century. Consistent with Figs. 2a, 3a model uncertainty (blue) is clearly dominant for all lead times considered, internal decadal variability (orange) is a significant factor at short lead times, and scenario uncertainty (green) only becomes important at the end of the century.

3 Sources of uncertainty on regional scales

Changes in global mean precipitation are not particularly relevant for decision makers. Instead, it is the changes on far smaller scales, and for different seasons, which are vital for adapting to a changing climate. For smaller regions, and for decadal means of particular seasons (Figs. 4b-d), the contribution from internal variability is larger, but

scenario uncertainty is generally still small, and in some cases, e.g. summer (JJA) Sahel rainfall (Fig. 4b), is completely negligible. European winter (DJF) rainfall (Fig. 4c) has a very large internal variability contribution, which is dominant until around 2050, likely related to the North Atlantic Oscillation (NAO). For JJA monsoon rainfall in South East Asia (Fig. 4d), scenario uncertainty is slightly larger than for the other regions shown, but internal variability and model uncertainty still dominate. A larger set of results for both temperature and precipitation can be viewed on our interactive website (http://ncas-climate.nerc.ac.uk/research/uncertainty/).

3.1 Uncertainty maps

We now further examine the sources of uncertainty on regional scales. We define 96 regions, each $30°$ wide in longitude with 8 varying thickness latitudinal bands to ensure each region has the same area (about 5×10^6 km^2). Fig. 5 shows maps of the fraction of variance explained by each source of uncertainty for these different regions and lead times, for both boreal winter (DJF, panel a) and summer (JJA, panel b).

It is clear that scenario uncertainty is rarely a significant source of uncertainty; the only exception is the polar regions at the end of the century. Model uncertainty dominates for nearly all regions for lead times longer than around four decades. At the end of the century, model uncertainty explains $60 - 95\%$ of the total uncertainty over virtually all regions away from the winter pole.

However, it must be noted that internal variability is the dominant source of uncertainty over all regions for the first decade ahead, many regions in the third decade ahead, and is of comparable importance to scenario uncertainty even at the end of the century. Internal climate fluctuations could therefore potentially mask or enhance, for a decade or so, the signal of anthropogenic changes. Appendix A shows that tropical Africa has especially large decadal variability relative to the mean precipitation.

By direct comparison with HS09, it is clear that both internal variability and model uncertainty are more important for precipitation changes than for temperature changes (as also found by Räisänen, 2001).

4 Signal-to-noise in precipitation projections

The signal-to-noise ratio (S/N) is often used to measure the robustness of a prediction. We now consider the S/N of these precipitation projections on regional scales,

$$\text{S/N} = \frac{\Delta_{\text{precip}}}{\sigma_{\text{precip}}}, \tag{1}$$

where Δ_{precip} is the change in decadal means of seasonal precipitation, relative to 1971-2000, and σ_{precip} is the total standard deviation of the projections. To assess the significance of the S/N, we consider the null hypothesis that the signal is zero. This null hypothesis can be rejected in favour of the hypothesis that the signal is non-zero at around the 8% significance level for a S/N of 2, using a t-test.

Maps of S/N are shown in Fig. 6a for boreal winter (DJF, top row) and summer (JJA, bottom row), for different lead times in the 21st century. The highest S/N is found in the polar regions where precipitation is projected to increase, and model uncertainty is relatively small. Away from the poles, there are few regions where the magnitude of S/N is above 1, even at the end of the century. Also, there are many areas where the magnitude of the S/N is less than 0.25, though this is often where the signal of precipitation changes is small.

For more populated areas, the Mediterranean is highlighted as having a relatively high S/N, for decreasing precipitation, especially in JJA. Central America also shows a relatively high S/N for decreasing precipitation in both JJA and DJF. North-eastern Europe, North Asia and Eastern Africa in DJF also show a relatively high S/N. Recently, Giorgi and Bi (2009) used the CMIP3 projections to find regions and lead times where the S/N was above 1. Although their methodology differs[3], the regions identified are similar.

In Fig. 6b we show the S/N for JJA precipitation, assuming zero model uncertainty, i.e. a 'potential S/N' assuming a perfect model, illustrating the potential gains from improving GCM representations of precipitation. The S/N increases are fairly modest, especially for the first 3 decades. Other seasons show similarly modest gains in S/N (not shown). This important point implies that even if all GCMs agreed on the ensemble mean precipitation change, this mean change is small relative to the internal variability, and this has implications for adaptation planners. Adapting to internal variability in precipitation is likely to aid successful adaptation to climate change in many regions for climate impacts that are seasonal mean precipitation dependent.

Fig. 6c shows the S/N for JJA temperature changes using the same methods. It is clear that S/N is far higher for temperature than for precipitation (also found by Murphy et al., 2004); other seasons (not shown) have similar S/N values. However, for temperature the S/N generally peaks in the mid-21st century and subsequently declines as scenario uncertainty becomes more important towards the end of the century. For precipitation, the maximum in S/N generally occurs much later in the 21st century, and for some regions is still increasing at 2100. Also, the tropical regions have the highest S/N for temperature changes, but among the lowest for precipitation changes. Fig. 6d shows the 'potential S/N' for JJA temperature, and demonstrates that the S/N could be increased considerably if model uncertainty was reduced, especially on adaptation timescales of up to 3 decades, in contrast with precipitation.

Finally, we consider how these findings may change if longer time means of precipitation are considered. Fig. 7 shows the S/N for a 30 year mean of JJA precipitation from 2020-2049 with (left) and without (right) model uncertainty. The S/N, and also the potential increase in S/N by narrowing model uncertainty, is larger in this example than for decadal means, suggesting that longer time means may need to be considered to ensure more robust projections of precipitation.

Note that these estimates of S/N assume that the signal is the mean change across all GCMs and scenarios, and the noise estimate relies heavily on the GCM estimates of

---

[3] Giorgi and Bi (2009) used 20 year means of precipitation changes for 6-month periods, and estimated the S/N for each scenario independently. We consider 10 year means for 3-month seasons and include the additional scenario uncertainty. It would therefore be expected that our methodology would produce lower S/N values, and this is indeed the case.

internal variability of precipitation. Appendix A shows a comparison of the GCM and observational estimates of decadal variability of precipitation and suggests that the GCMs may underestimate its magnitude. If this is the case, then our estimated S/N would be an upper limit, although there is also considerable uncertainty in the observed estimates.

5 Conclusions and discussion

We have separated and quantified the three sources of uncertainty in global and regional projections of precipitation change for the 21st century. Our main findings are as follows:

1. Internal variability contributes 50-90% of the total uncertainty for all regions for precipitation projections of the next decade, and is the most important uncertainty for many regions for lead times up to 30 years. Model uncertainty is generally dominant thereafter. Scenario uncertainty is generally small or negligible over land areas.
2. The signal-to-noise of precipitation projections is highest near the poles (often > 3 by the end of the century), but is far lower than for temperature everywhere. This is especially true for the tropics where S/N is highest for temperature (often > 4 in mid-century) but close to zero for precipitation. Outside of the polar regions, the projected decreases in Mediterranean and Central American precipitation show the highest S/N (> 2 by the end of the century), consistent with the findings of Giorgi and Bi (2009).
3. The potential gains in S/N from reducing model uncertainty to zero are modest for predictions of decadal mean precipitation change, especially for predictions of the next few decades, implying that adaptation decisions will need to be made in the context of high uncertainty. For longer time means of precipitation and for decadal mean temperature, the potential to reduce uncertainty is far greater.

This type of analysis also has important consequences for modelling the impacts of precipitation change. For policy relevant advice, it is vital that studies on the impacts of climate change consider a wide range of GCMs (e.g., Wilby and Harris, 2006; Poulter et al., 2009). If not, there is a significant risk of underestimating the total uncertainty in impacts predictions. The low signal-to-noise values of current precipitation projections also have important implications for adaptation, e.g. for decisions on investment in infrastructure such as reservoirs. Robust decisions need to be made soon (e.g., Dessai and Hulme, 2007), and reduced uncertainty would allow better decisions, but a substantial reduction in uncertainty for precipitation predictions of the next few decades seems unlikely in the near future. However, for temperature there is a larger potential to reduce uncertainty (Figs. 6c,d). Lobell and Burke (2008) recently showed that uncertainties in crop yield predictions in most regions were dominated by uncertainties in future temperature, rather than precipitation, because the projected changes in temperature are further outside the range of present-day internal variability. Thus there is real potential to reduce uncertainty in some climate impact predictions through GCM improvement.

It is important to note that the identified dominant sources of uncertainty (i.e. model uncertainty and internal variability) are potentially reducible through progress in climate science. Reducing model uncertainty in precipitation requires the continued improvement of the representation of the hydrological cycle in climate models. However, our results suggest that this reduction in model uncertainty would only give substantially more confident

precipitation predictions for mid-late 21st century because of the considerable internal variability, relative to the signal, for the next few decades. Note that there is some evidence that predictions of higher order precipitation statistics (e.g., extremes), which are often more important for climate impacts, may have greater confidence than the seasonal means discussed here (see e.g. Tebaldi et al., 2006).

Decadal climate forecasts which are initialised from the observed state of the ocean (Smith et al., 2007; Keenlyside et al., 2008; Pohlmann et al., 2009) are designed to predict some of the internal variability component of precipitation for a few years ahead, especially in regions such as the Sahel, North America and western Europe, where the role of the nearby ocean state is particularly important (e.g., Sutton and Hodson, 2005), but this potential has yet to be explored in detail. These initialised forecasts also have the potential to reduce the model uncertainty component of uncertainty by, firstly, starting the models from similar climate states and thus reducing the model spread for short lead times, and secondly, examining how and why the models diverge from the subsequent observations may allow the processes responsible to be identified and their representations improved. The initialised decadal predictions planned for the next Coupled Model Intercomparison project (CMIP5; Meehl et al., 2009) offer a new opportunity to explore these issues, and will also allow analysis of the important relationships between the 'spread' in climate projections (as considered here) and the 'skill' in climate predictions. Research in weather and seasonal forecasting has shown that the relationships between prediction spread and prediction skill are rarely straightforward, but there is little published work on these relationships for longer lead time climate predictions, although Palmer et al. (2008) describe one way of calibrating long lead time predictions using the reliability of seasonal forecasts.

The small contribution of scenario uncertainty is also worthy of further comment. Although studies may find significant changes in the regional precipitation response for different scenarios using a single GCM, it is likely that using a different GCM would give a far larger change, and inter-scenario differences of a single GCM should not be over-interpreted. However, the response to aerosol forcings, which have a large spatial variations and short atmospheric lifetime may be an exception to this generalisation.

Finally, it is necessary to consider whether these conclusions might change for a future range of GCMs, especially as we have not considered uncertainty due to model biases, or errors, that are common to all current GCMs. For example, Atlantic 'blocking' is not generally well simulated in GCMs at present and this common model error may impact the conclusions drawn from Fig. 4c. The generally higher resolution GCMs being prepared for CMIP5 may simulate blocking and other aspects of the climate system better, and provide different quantitative estimates of the uncertainty. However, it seems unlikely that model uncertainty will decrease dramatically for the new generation of GCMs, and it is even likely that model uncertainty will increase for predictions on multi-decadal lead times due to the incorporation of additional Earth system feedbacks, e.g. the carbon cycle (Knutti et al., 2008) or land use changes (Feddema et al., 2005). Our conclusions on the potential S/N of projections without model uncertainty also depend on the mean response of the GCMs considered and on the simulation of precipitation variability; how this will change for a new generation is not known, though the pattern of the mean precipitation response

did not change considerably between the 3rd and 4th IPCC assessment reports. Lastly, it is worth noting that the CMIP3 GCMs should probably not be considered as independent models, and therefore the 'spread' between models may need inflating (e.g., Jewson and Hawkins, 2009).

Appendix A

A.1 Testing the internal variability estimates

We test our estimates of the internal variability component of regional precipitation using the constant forcing pre-industrial control integrations of the same GCMs, in which there are no complicating transient forcing effects to consider[4]. This estimate can then be compared to the estimate derived from the transient integrations.

Fig. 8 shows the standard deviation of running decadal means of regional precipitation, expressed as a percentage of the mean precipitation, for both the pre-industrial control integrations (panel a) and the 21st century transient integrations (panel b). The patterns are very similar, giving us confidence in our estimates of the decadal variability component of the uncertainty.

Boer (2009) also analysed the CMIP3 pre-industrial control integrations and found that the magnitude of the zonal mean decadal variability, relative to the mean precipitation, peaks in the tropics, and increases slightly with increased radiative forcings. The maps in Fig. 8 suggest that it is Africa which dominates the estimates of zonal mean decadal variability in the tropics, and the Sahel region is well known to have large decadal variability in precipitation (e.g., Rowell et al., 1995), possibly caused by changes in the Atlantic Multi-decadal Oscillation (AMO) (e.g., Folland et al., 1986).

A.2 Comparison with observational estimates

Fig. 8c shows an estimate of the decadal variability from the CRU TS3.0 observational dataset (Mitchell and Jones, 2005) for 1901-2006, calculated in a similar way to the GCM estimates above. The observations consist of land-only annual mean data, have been re-gridded onto a $10° \times 10°$ grid, and detrended with a fourth order polynomial. Note that the scale on Fig. 8c is twice that of Figs. 8a,b. The regions identified as having relatively large decadal variability are similar to the GCMs, but this analysis suggests that the observed decadal variability in precipitation is larger than the GCM estimates, although it must be noted that the observational estimate will have considerable uncertainties. Zhang

---

[4] Note however that some GCMs show a drift in precipitation related to the spin-up of the model. This drift is removed using a second order polynomial.

et al. (2007) also found that for land-only zonal means, the variability in precipitation was significantly underestimated in GCMs when compared to observations, but Boer (2009) found that the internal variability of the GCMs agreed well with an observational estimate of zonal mean precipitation. There is therefore a suggestion, but certainly no consensus, that GCMs may underestimate the magnitude of decadal variability in precipitation.

Appendix B

In Fig. 2 we show the proportion of the total standard deviation due to each type of uncertainty. This has been estimated by considering that the total variance in the projections (T^2) is the sum of the variance due to internal variability (I^2), model uncertainty (M^2) and scenario uncertainty (S^2),

$$T^2 = I^2 + M^2 + S^2. \tag{2}$$

When considering the total standard deviation, T, we would like,

$$T = I' + M' + S' = \frac{I}{F} + \frac{M}{F} + \frac{S}{F}, \tag{3}$$

where the primes denote scaled versions of I, M and S. The common scaling factor, F, is then,

$$F = \frac{I + M + S}{T} \tag{4}$$

and the boundaries between the different coloured sections in Fig. 2 are at $\frac{\pm I}{F}, \frac{\pm(I+M)}{F}$ and $\frac{\pm(I+M+S)}{F}$.

References

Adler RF, Huffman GJ, Chang A, Ferraro R, Xie P, Janowiak J, Rudolf B, Schneider U, Curtis S, Bolvin D, Gruber A, Susskind J, Arkin P (2003) The Version 2 Global Precipitation Climatology Project (GPCP) Monthly Precipitation Analysis (1979-Present). J Hydrometeor 4: 1147–1167

Boer GJ (2009) Changes in interannual variability and decadal potential predictability under global warming. J Climate 22: 3098–3109 doi:10.1175/2008JCLI2835.1

Brohan P, Kennedy JJ, Harris I, Tett SFB, Jones P (2006) Uncertainty estimates in regional and global observed temperature changes: a new dataset from 1850. J Geophys Res 111: D12106 doi:10.1029/2005JD006548

Dessai S, Hulme M (2007) Assessing the robustness of adaptation decisions to climate change uncertainties: a case study on water resources management in the East of England. Glob Env Change 17: 59–72 doi:10.1016/j.gloenvcha.2006.11.005

Feddema JJ, Oleson KW, Bonan GB, Mearns LO, Buja LE, Meehl GA, Washington WM (2005) The importance of land-cover change in simulating future climates. Science 310: 1674–1678 doi:10.1126/science.1118160

Folland CK, Palmer TN, Parker DE (1986) Sahel rainfall and worldwide sea temperatures, 1901-85. Nature 320: 602–607 doi:10.1038/320602a0

Giorgi F, Bi X (2009) Time of emergence (TOE) of GHG-forced precipitation change hot-spots. Geophys Res Lett 36: L06709 doi:10.1029/2009GL037593

Giorgi F, Mearns LO (2002) Calculation of average, uncertainty range, and reliability of regional climate changes from AOGCM simulations via the Reliability Ensemble Averaging (REA) method. J Clim 1141–1158

Harris G, Sexton D, Booth B, Collins M, Murphy J, Webb M (2006) Frequency distributions of transient regional climate change from perturbed physics ensembles of general circulation model simulations. Clim Dyn 27: 357–375 doi:10.1007/s00382-006-0142-8

Hawkins E, Sutton R (2009) The potential to narrow uncertainty in regional climate predictions. Bull Amer Met Soc 90: 1095–1107 doi:10.1175/2009BAMS2607.1

Jewson S, Hawkins E (2009) CMIP3 ensemble spread, model similarity, and climate prediction uncertainty available from http://arxiv.org/abs/0909.1890

Keenlyside NS, Latif M, Jungclaus J, Kornblueh L, Roeckner E (2008) Advancing decadal-scale climate prediction in the North Atlantic sector. Nature 453: 84–88 doi: 10.1038/nature06921

Knutti R, Allen MR, Friedlingstein P, Gregory JM, Hegerl GC, Meehl GA, Meinshausen M, Murphy JM, Plattner GK, Raper SCB, Stocker TF, Stott PA, Teng H, Wigley TML (2008) A review of uncertainties in global temperature projections over the twenty-first century. J Climate 21: 2651–2663 doi:10.1175/2007JCLI2119.1

Lobell DB, Burke MB (2008) Why are agricultural impacts of climate change so uncertain? The importance of temperature relative to precipitation. Environ Res Lett 3: 034 007 doi:10.1088/1748-9326/3/3/034007

Meehl GA, Goddard L, Murphy J, Stouffer RJ, Boer G, Danabasoglu G, Dixon K, Giorgetta MA, Greene AM, Hawkins E, Hegerl G, Karoly D, Keenlyside N, Kimoto M, Kirtman B, Navarra A, Pulwarty R, Smith D, Stammer D, Stockdale T (2009) Decadal prediction: can it be skillful? Bull Amer Met Soc 90: 1467–1485 doi: 10.1175/2009BAMS2607.1

Meehl GA, Stocker TF, Collins W, Friedlingstein P, Gaye AT, Gregory JM, Kitoh A, Knutti R, Murphy JM, Noda A, Raper SCB, Watterson IG, Weaver AJ, Zhao ZC Global climate projections. In: Climate Change 2007: The Physical Science Basis. Contribution of Working Group I to the Fourth Assessment Report of the Intergovernmental Panel on Climate Change Cambridge University Press, Cambridge, UK. 2007

Mitchell TD, Jones PD (2005) An improved method of constructing a database of monthly climate observations and associated high-resolution grids. Int J Climatology 25: 693–712 doi:10.1002/joc.1181

Murphy JM, Sexton DMH, Barnett DN, Jones GS, Webb MJ, Collins M, Stainforth DA (2004) Quantification of modelling uncertainties in a large ensemble of climate change simulations. Nature 430: 768–772 doi:10.1038/nature02771

Palmer TN, Doblas-Reyes FJ, Weisheimer A, Rodwell MJ (2008) Towards seamless prediction: calibration of climate change projections using seasonal forecasts. Bull Amer Met Soc 89: 459–470 doi:10.1175/BAMS-89-4-459

Pohlmann H, Jungclaus J, Kohl A, Stammer D, Marotzke J (2009) Initializing decadal climate predictions with the GECCO oceanic synthesis: Effects on the North Atlantic. J Climate 22: 3926–3938 doi:10.1175/2009JCLI2535.1

Poulter B, Hattermann F, Hawkins E, Zaehle S, Sitch S, Restrepo-Coupe N, Heyder U, Cramer W (2009) Robust dynamics of Amazon dieback to climate change with perturbed ecosystem model parameters. Glob Change Bio in press

Räisänen J (2001) CO_2-induced climate change in CMIP2 experiments: quantification of agreement and role of internal variability. J Climate 14: 2088–2104

Rowell DP, Folland CK, Maskell K, Ward MN (1995) Variability of summer rainfall over tropical north Africa (1906-92): Observations and modelling. Q J Royal Met Soc 121: 669 – 704

Smith DM, Cusack S, Colman AW, Folland CK, Harris GR, Murphy JM (2007) Improved surface temperature prediction for the coming decade from a global climate model. Science 317: 796–799 doi:10.1126/science.1139540

Stainforth DA, Aina T, Christensen C, Collins M, Faull N, Frame DJ, Kettleborough JA, Knight S, Martin A, Murphy JM, Piani C, Sexton D, Smith LA, Spicer RA, Thorpe AJ, Allen MR (2005) Uncertainty in the predictions of the climate response to rising levels of greenhouse gases. Nature 433: 403–406 doi:10.1038/nature03301

Sutton RT, Hodson DLR (2005) Atlantic Ocean forcing of North American and European summer climate. Science 309: 115–118 doi:10.1126/science.1109496

Tebaldi C, Hayhoe K, Arblaster JM, Meehl GA (2006) Going to the Extremes: An Intercomparison of Model-Simulated Historical and Future Changes in Extreme Events. Clim Change 79: 185–211 doi:10.1007/s10584-006-9051-4

Tebaldi C, Mearns LO, Nychka D, Smith RL (2004) Regional probabilities of precipitation change: A Bayesian analysis of multimodel simulations. Geophys Res Lett 31: L24 213 doi:10.1029/2004GL021276

Wilby RL, Harris I (2006) A framework for assessing uncertainties in climate change impacts: Low-flow scenarios for the River Thames, UK. Water Resources Res 42: W02 419 doi:10.1029/2005WR004065

Zhang X, Zwiers FW, Hegerl GC, Lambert FH, Gillett NP, Solomon S, Stott PA, Nozawa T (2007) Detection of human influence on twentieth-century precipitation trends. Nature 448: 461–465 doi:10.1038/nature06025

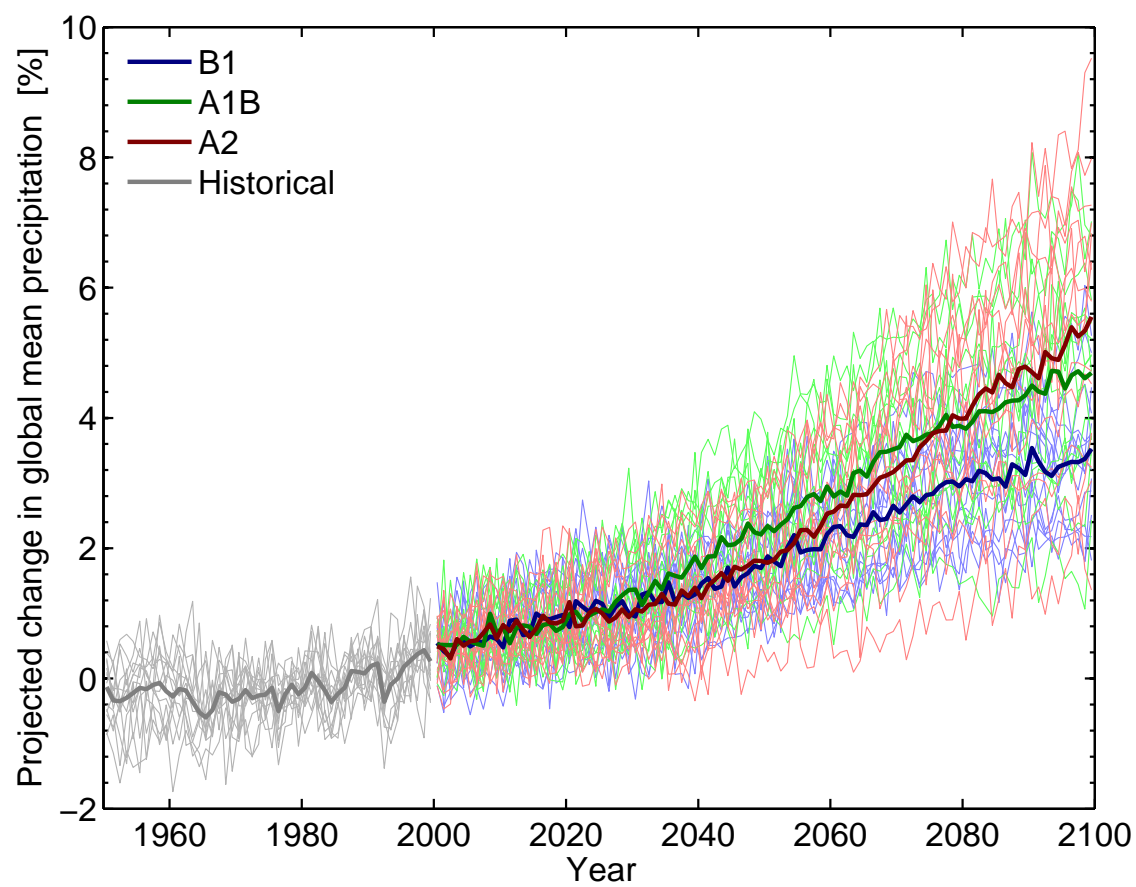**Fig. 1** CMIP3 projections of changes in global mean precipitation, relative to the mean of 1971-2000, for historical forcings and different future emission scenarios. The different lines each represent a different global climate model for SRES B1 (blue), A1B (green) and A2 (red) scenarios, with historical projections shown in grey. The thick lines represent the multi-model means for each scenario.
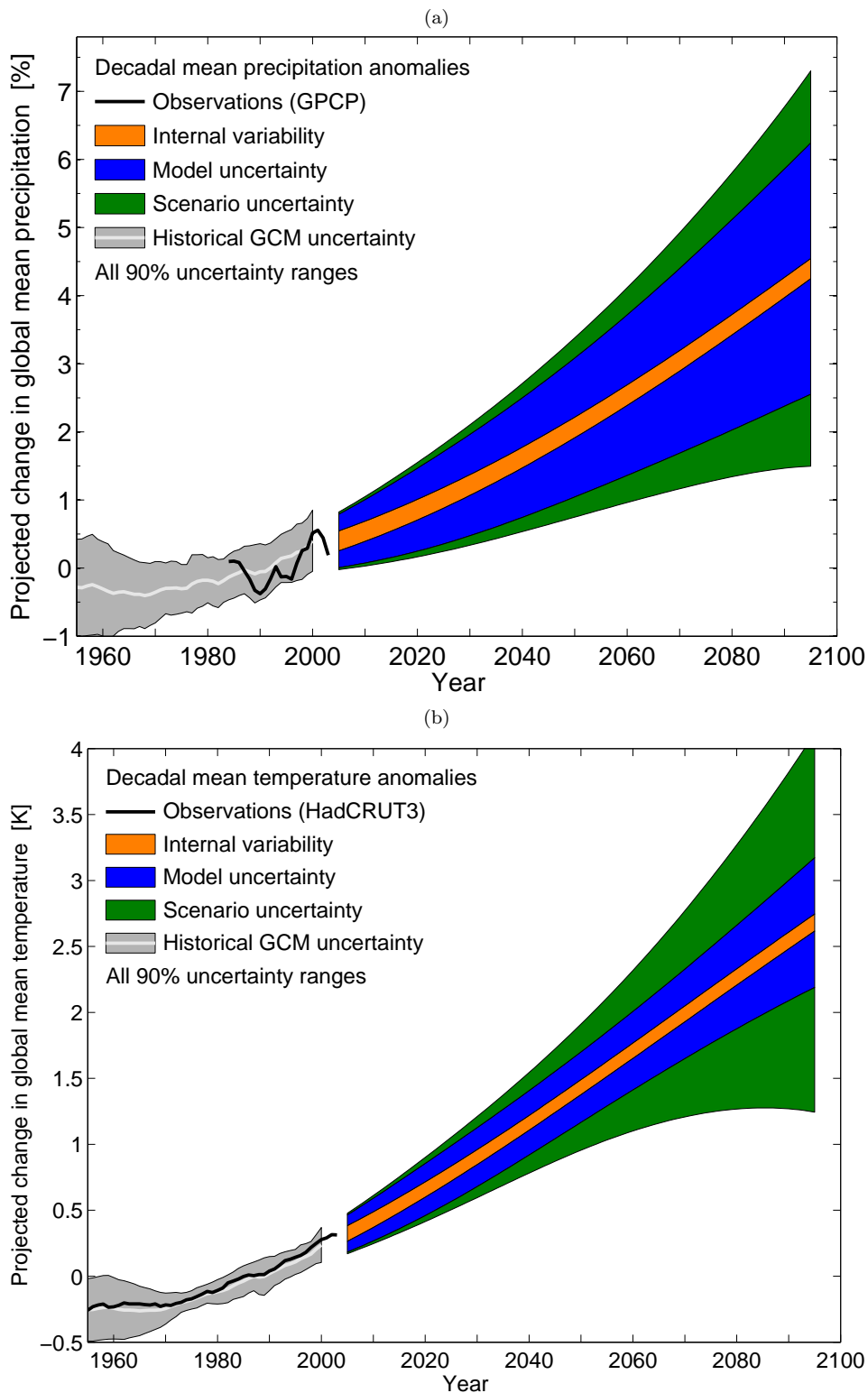
Fig. 2 The total uncertainty in CMIP3 global mean, decadal mean projections for the 21st century, separated into its three components: internal variability (orange), model uncertainty (blue) and scenario uncertainty (green). The grey regions show the uncertainty in the 20th century integrations of the same GCMs, with the mean in white. The black lines show an estimate of the observed historical changes. (a) Precipitation, with observations from GPCP v2.1 (Adler et al., 2003). (b) Temperature, with observations from HadCRUT3 (Brohan et al., 2006). All anomalies are calculated relative to the 1971-2000 mean, except for the precipitation observations, for which a 1979-2000 mean is used. Appendix B describes how the components of standard deviation were scaled from the estimated variances.
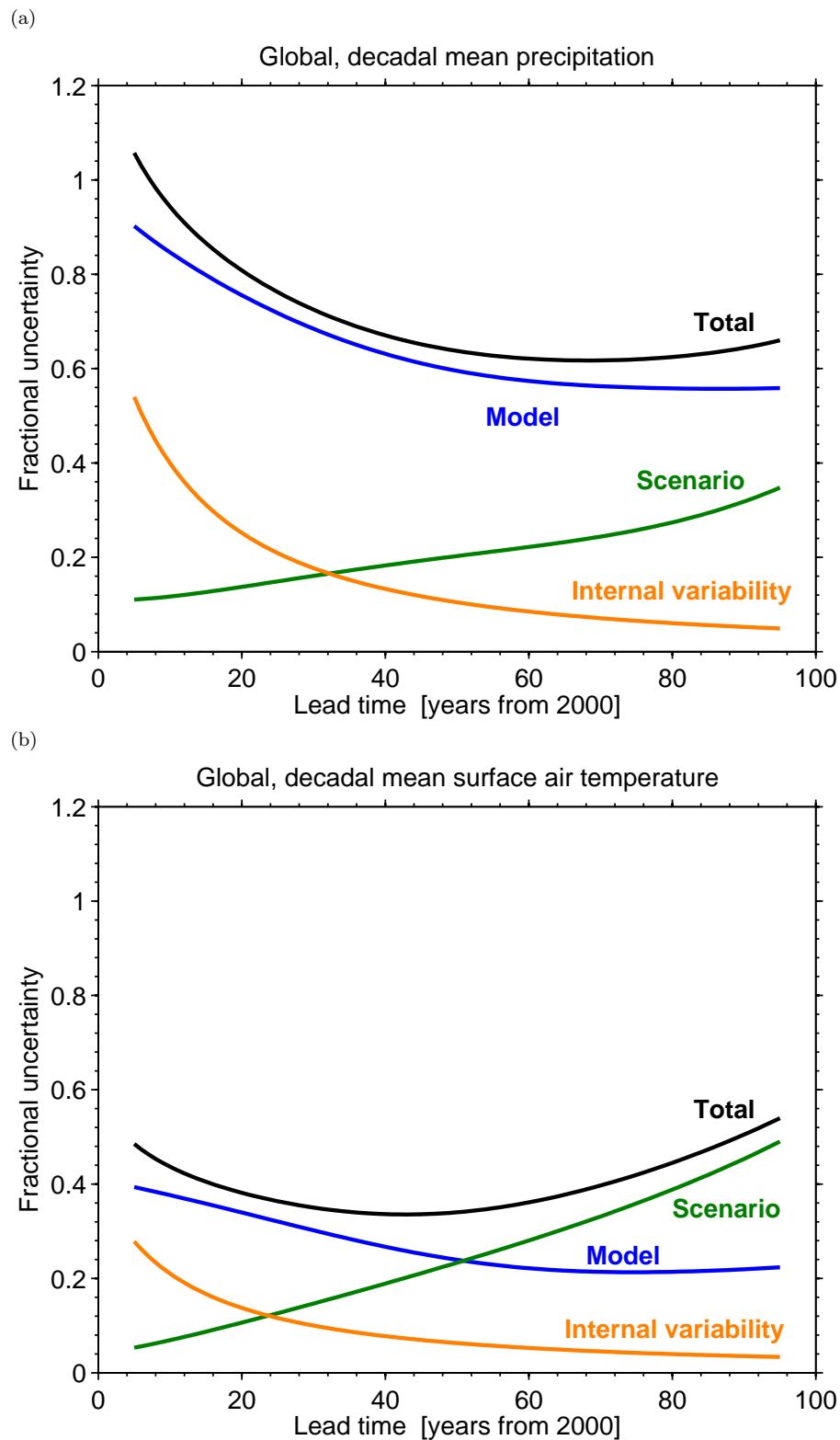
(a)

(b)

Fig. 3 The fractional uncertainty in decadal mean, global mean climate projections, defined as the uncertainty divided by the expected mean change for (a) precipitation, and (b) surface air temperature (after HS09).
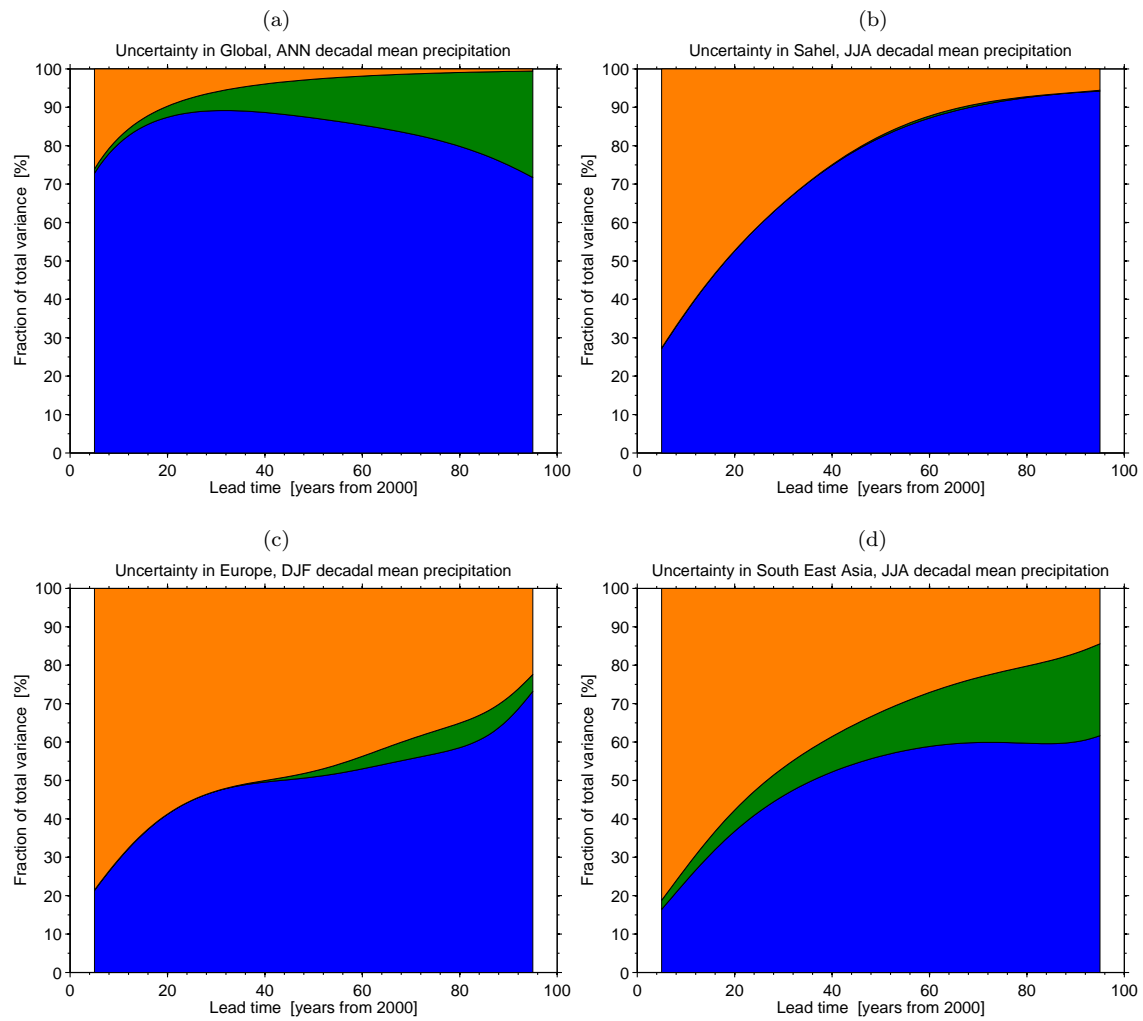
(a)

Uncertainty in Global, ANN decadal mean precipitation

(b)

Uncertainty in Sahel, JJA decadal mean precipitation

(c)

Uncertainty in Europe, DJF decadal mean precipitation

(d)

Uncertainty in South East Asia, JJA decadal mean precipitation

Fig. 4 Fraction of total variance in decadal mean precipitation projections explained by internal variability (orange), model uncertainty (blue) and scenario uncertainty (green), for (a) global, annual mean, (b) Sahel JJA mean, (c) European DJF mean, and (d) South East Asian JJA mean.

Fig. 5 Fraction of variance explained by the three sources of uncertainty in projections of decadal mean seasonal precipitation changes, for (a) boreal winter (DJF), and (b) boreal summer (JJA). Each grid cell has the same area, roughly 5×10^6 km^2.
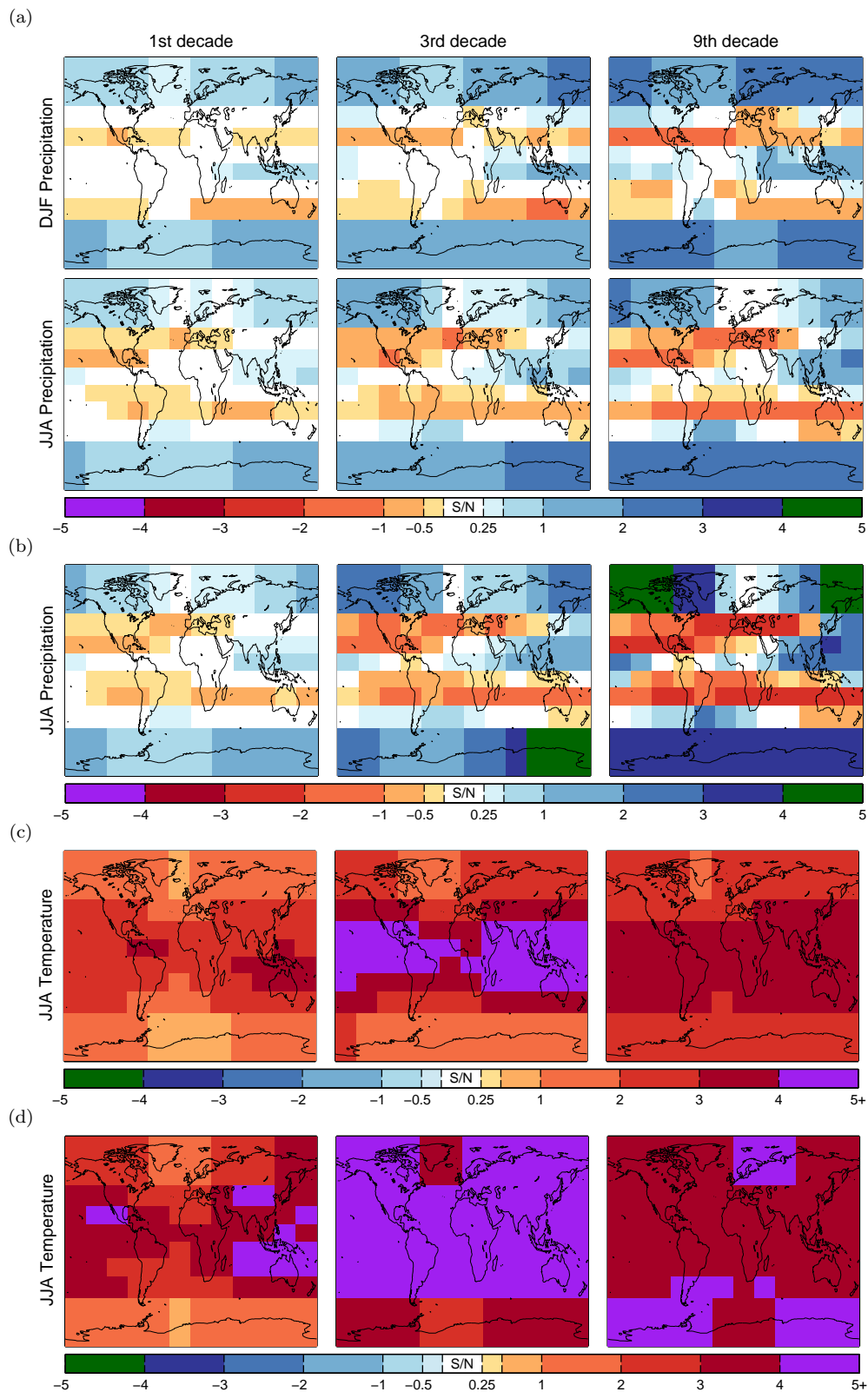
Fig. 6 Signal-to-noise (S/N) ratio for projections of decadal mean seasonal climate changes for, (a) precipitation (DJF, top row and JJA, bottom row), (b) precipitation for JJA, but assuming model uncertainty is zero, (c) surface air temperature for JJA, and (d) surface air temperature for JJA, but assuming model uncertainty is zero. Note the reversed colour scale for temperature. A negative S/N denotes where precipitation is projected to decrease.
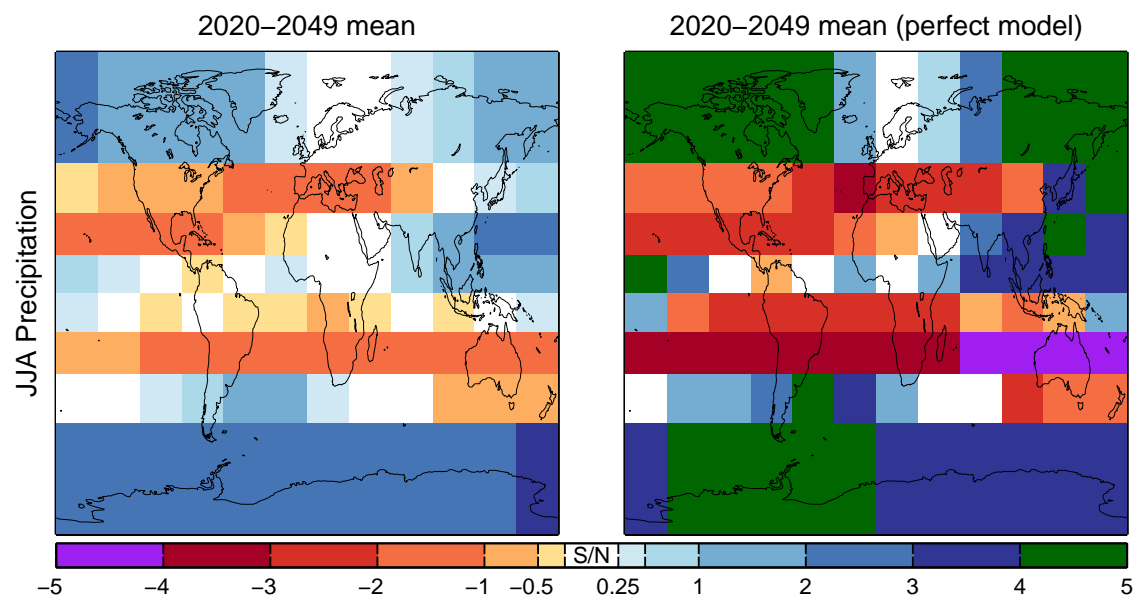
Fig. 7 Signal-to-noise ratio for projections of JJA precipitation changes for a 30-year mean period (2020-2049) with (left) and without (right) model uncertainty.
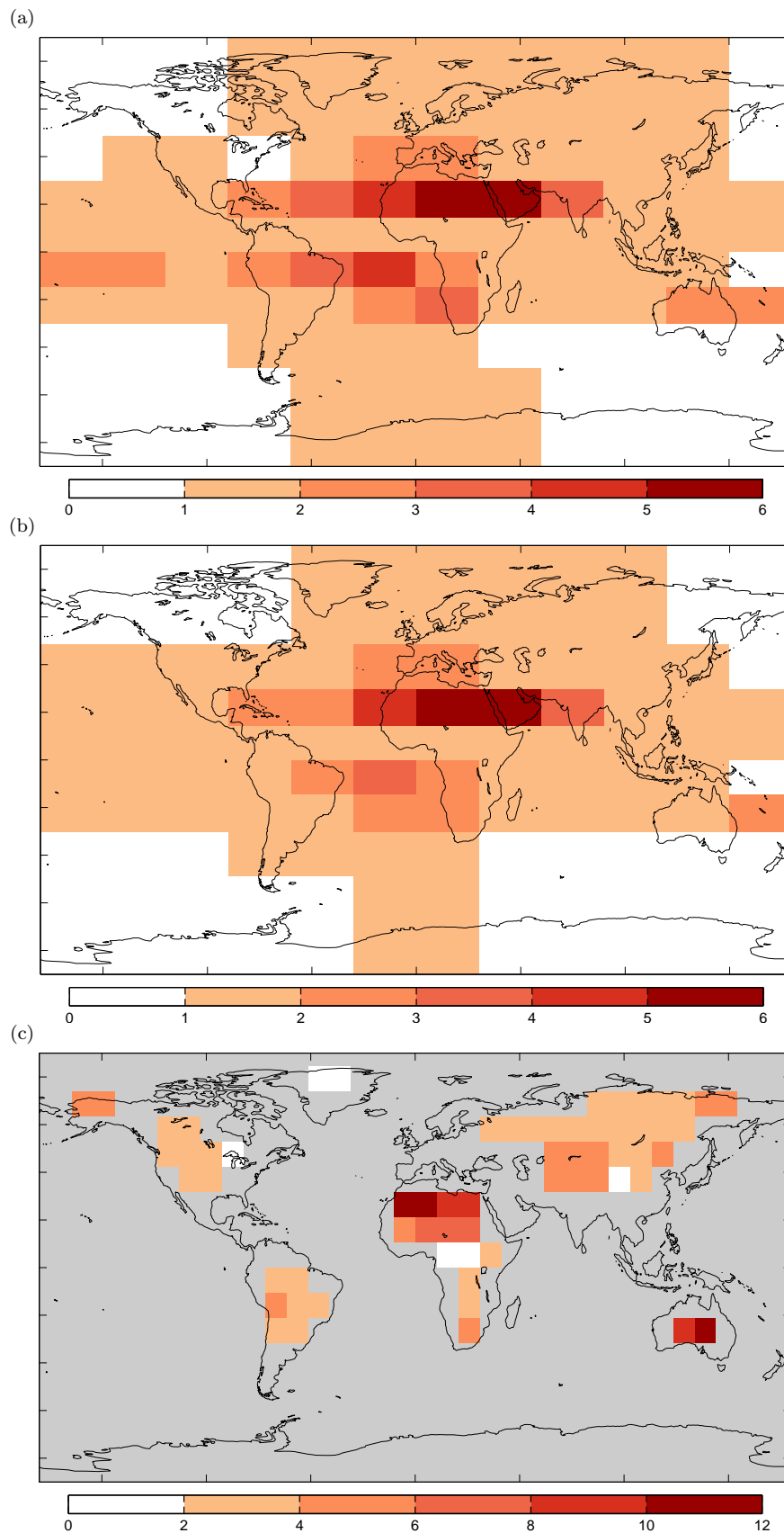
(a)

(b)

(c)

Fig. 8 Estimates of the decadal internal variability of regional precipitation. (a) Mean standard deviation from the pre-industrial control integrations of the GCMs used. (b) Mean standard deviation for the 21st century integrations of the GCMs used. (c) From the CRU TS3.0 land observations for 1901-2006 (Mitchell and Jones, 2005), averaged into 10° boxes, using a 1971-2000 climatology. Grey denotes no data. Note the different colour scale for the observations. Units are % of the mean precipitation.